

Multi-phase Synchronous Motors: POG Modeling and Optimal Shaping of the Rotor Flux

Roberto Zanasi, Federica Grossi

DII, University of Modena and Reggio Emilia, Modena, Italy, (e-mail: roberto.zanasi@unimo.it)

Abstract—In the paper the Power-Oriented Graphs (POG) technique is used for modelling m -phase permanent magnet synchronous motors and a study on the rotor flux is given. The POG model of the considered electrical motor shows its internal structure from a “power” point of view. The dynamic model of the motor is as general as possible and it considers an arbitrary odd number of phases. Generalized orthonormal transformations allow to write the dynamic equations of the system in a very compact form. The rotor flux is analyzed, in particular in order to minimize currents needed for the torque generation. An optimal shape for the rotor flux is presented. The model is finally implemented in Matlab/Simulink and some simulations are carried out.

I. INTRODUCTION

In this paper the dynamic model of a permanent magnet synchronous electric motor is obtained using the modeling technique named “Power-Oriented Graphs” (POG), see [1] and [2]. The obtained POG graphical representation shows very well the internal structure of the motors from a “power” point of view: the electric part of the motor interacts with the mechanical one by means of a “connection” block which neither store nor dissipate energy. With a proper choice of the reference frame, the dynamic model of the electric motor becomes very simple and clear. To obtain the dynamic model of the motors, a Lagrangian approach has been used.

The paper is organized as follows. Section II states the basic properties of the POG modelling technique. Section III shows the details of POG modelling of n -phase permanent magnet synchronous motors and the study of the rotor flux in order to minimize currents needed for the torque generation. Finally, in Section IV some simulations are reported.

A. Notations

In the paper the following notations will be used:

- Row matrices:

$$\llbracket R_i \rrbracket = \begin{bmatrix} R_1 & R_2 & \dots & R_n \end{bmatrix}_{1:n}$$

- Column and diagonal matrices:

$$\llbracket R_i \rrbracket = \begin{bmatrix} R_1 \\ R_2 \\ \vdots \\ R_n \end{bmatrix}_{1:n}, \quad \llbracket R_i \rrbracket = \begin{bmatrix} R_1 & & & \\ & R_2 & & \\ & & \ddots & \\ & & & R_n \end{bmatrix}$$

- Full matrices:

$$\llbracket R_{i,j} \rrbracket = \begin{bmatrix} R_{11} & R_{12} & \dots & R_{1m} \\ R_{21} & R_{22} & \dots & R_{2m} \\ \vdots & \vdots & \ddots & \vdots \\ R_{n1} & R_{n2} & \dots & R_{nm} \end{bmatrix}$$

- The symbol

$$\sum_{n=a:d}^b c_n = c_a + c_{a+d} + c_{a+2d} + c_{a+3d} + \dots$$

will be used for representing the sum of a succession of numbers c_n , where the index n ranges from a to b with increment d that is, using the Matlab notation, $n = [a:d:b]$.

II. THE BASES OF POWER-ORIENTED GRAPHS

The “Power-Oriented Graphs” are “signal flow graphs” combined with a particular “modular” structure which essentially uses only the two blocks shown in Fig. 1. The basic characteristic of this modular structure is the direct correspondence between pairs of system variables and real power flows: the product of the two variables involved in each dashed line of the graph has the physical meaning of “power flowing through the section”. The two basic blocks

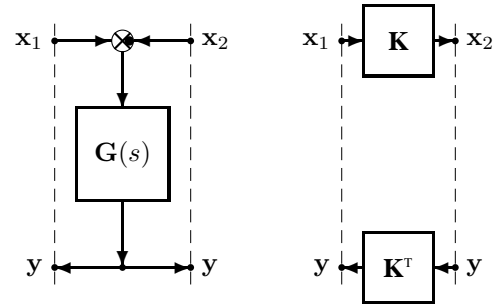


Fig. 1. Basic blocks: elaboration block (e.b.) and connection block (c.b.).

shown in Fig. 1 are named “elaboration block” (e.b.) and “connection block” (c.b.). The circle present in the e.b. is a summation element and the black spot represents a minus sign that multiplies the entering variable. There is no restriction on variables x and y other than the fact that their inner product $\langle x, y \rangle = x^T y$ must have the physical meaning of a “power”. The e.b. and the c.b. are suitable for representing both scalar and vectorial systems. In the vectorial case, $G(s)$ and K are matrices: $G(s)$ is always square, K can also be rectangular. While the elaboration

block can store and dissipate energy (i.e. springs, masses and dampers), the connection block can only “transform” the energy, that is, transform the system variables from one type of energy-field to another (i.e. any type of gear reduction). In the linear vectorial case when $\mathbf{G}(s) = [\mathbf{M}s + \mathbf{R}]^{-1}$, (\mathbf{M} is symmetric and positive definite) the energy E_s stored in the e.b. and the power P_d dissipating in the e.b. can be expressed as:

$$E_s = \frac{1}{2} \mathbf{y}^T \mathbf{M} \mathbf{y}, \quad P_d = \mathbf{y}^T \mathbf{R} \mathbf{y}.$$

There is a direct correspondence between the POG representations and the corresponding state space descriptions. For example, the system

$$\begin{cases} \mathbf{L} \dot{\mathbf{x}} = \mathbf{A} \mathbf{x} + \mathbf{B} \mathbf{u} \\ \mathbf{y} = \mathbf{B}^T \mathbf{x} \end{cases} \quad \mathbf{L} = \mathbf{L}^T > 0 \quad (1)$$

can be represented by the POG scheme shown in Fig. 2.

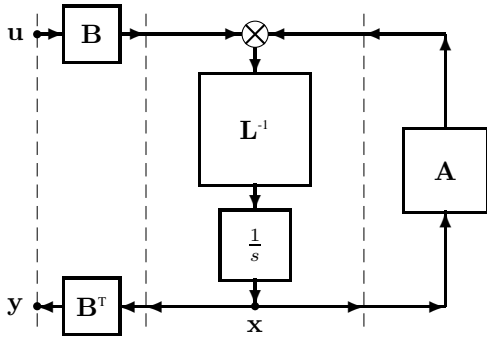


Fig. 2. POG block scheme of a generic dynamic system.

When an eigenvalue of matrix \mathbf{L} tends to zero (or to infinity), system (1) degenerates towards a lower dimension dynamic system. In this case, the dynamic model of the “reduced” system can be directly obtained from (1) by using a simple “congruent” transformation $\mathbf{x} = \mathbf{T} \mathbf{z}$ (\mathbf{T} is constant):

$$\begin{cases} \mathbf{T}^T \mathbf{L} \mathbf{T} \dot{\mathbf{z}} = \mathbf{T}^T \mathbf{A} \mathbf{T} \mathbf{z} + \mathbf{T}^T \mathbf{B} \mathbf{u} \\ \mathbf{y} = \mathbf{B}^T \mathbf{T} \mathbf{z} \end{cases} \Leftrightarrow \begin{cases} \bar{\mathbf{L}} \dot{\mathbf{z}} = \bar{\mathbf{A}} \mathbf{z} + \bar{\mathbf{B}} \mathbf{u} \\ \mathbf{y} = \bar{\mathbf{B}}^T \mathbf{z} \end{cases}$$

where $\bar{\mathbf{L}} = \mathbf{T}^T \mathbf{L} \mathbf{T}$, $\bar{\mathbf{A}} = \mathbf{T}^T \mathbf{A} \mathbf{T}$ and $\bar{\mathbf{B}} = \mathbf{T}^T \mathbf{B}$. If matrix \mathbf{T} is time-varying, an additional term $\mathbf{T}^T \dot{\mathbf{L}} \mathbf{T} \mathbf{z}$ appears in the transformed system. When matrix \mathbf{T} is rectangular, the system is transformed and reduced at the same time.

III. ELECTRICAL MOTORS MODELLING

In the paper the dynamic model of a permanent magnet synchronous electric motor is obtained using the modeling technique named “Power-Oriented Graphs” (POG). In particular we will refer only to permanent magnet synchronous electrical motors with an *odd* number m of phases. The considered multi-phase electrical motor is characterized by the following parameters:

- m : number of motor phases;
- p : number of polar expansions;
- θ, θ_r : electric and rotor angular positions: $\theta = p \theta_r$;
- ω, ω_r : electric and rotor angular velocities: $\omega = p \omega_r$;
- N_c : number of coils for each phase;
- R_i : i -th phase resistance ($p = 1$);
- L_i : i -th phase self induction coefficient ($p = 1$);
- M_{ij} : mutual induction coefficient of i -th phase coupled with j -th phase ($p = 1$);
- $\phi(\theta)$: rotor permanent magnet flux;
- $\phi_c(\theta)$: total rotor flux chained with stator phase 1;
- $\phi_{ci}(\theta)$: total rotor flux chained with stator phase i -th;
- φ_r : maximum value of function $\phi(\theta)$;
- φ_c : maximum value of function $\phi_c(\theta)$;
- J_r : rotor inertia momentum;
- b_r : rotor linear friction coefficient;
- τ_r : electromotive torque acting on the rotor;
- τ_e : external load torque acting on the rotor;
- γ : basic angular displacement;

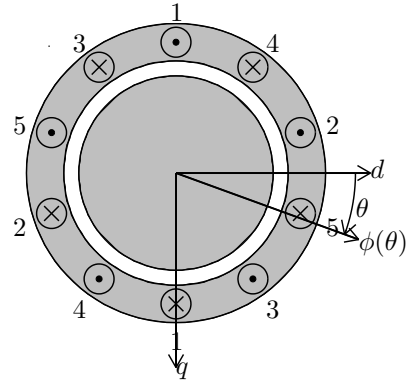


Fig. 3. Structure of a five-phase motor in the case of single polar expansion ($p = 1$).

Fluxes $\phi(\theta)$ and $\phi_c(\theta)$ satisfy the relation:

$$\phi_c(\theta) = p N_c \phi(\theta) = p N_c \varphi_r \bar{\phi}(\theta) = \varphi_c \bar{\phi}(\theta)$$

where $\varphi_c = p N_c \varphi_r$ and $\bar{\phi}(\theta)$ is the rotor flux function normalized with respect to its maximum value φ_r .

Let $\gamma = \frac{2\pi}{m}$ denote the basic angular phase displacement for electrical motors with m phases. The following hypotheses are assumed:

- H1) Function $\phi(\theta)$ is periodic with period 2π ;
- H2) Function $\phi(\theta)$ is an even function of θ ;
- H3) Function $\phi(\theta + \frac{\pi}{2})$ is an odd function of θ ;
- H4) For $\theta = 0$ the rotor flux $\phi_c(\theta)$ chained with phase 1 is maximum;
- H5) The electrical motor is homogeneous in its electrical characteristics.

Let us introduce the state vectors $\dot{\mathbf{q}}$, \mathbf{q} and the generalized flux vector $\Phi(\mathbf{q})$:

$$\dot{\mathbf{q}} = \begin{bmatrix} \mathbf{I} \\ \omega \end{bmatrix}, \quad \mathbf{q} = \begin{bmatrix} \mathbf{Q} \\ \theta \end{bmatrix}, \quad \Phi(\mathbf{q}) = \begin{bmatrix} \Phi_c(\theta) \\ 0 \end{bmatrix}$$

where \mathbf{I} and Φ_c are the current and flux vectors:

$$\mathbf{I} = \begin{bmatrix} I_1 \\ I_2 \\ \vdots \\ I_m \end{bmatrix}, \quad \Phi_c(\theta) = \begin{bmatrix} \phi_{c1}(\theta) \\ \phi_{c2}(\theta) \\ \vdots \\ \phi_{cm}(\theta) \end{bmatrix} = \begin{bmatrix} \phi_c(\theta) \\ \phi_c(\theta - \gamma) \\ \phi_c(\theta - 2\gamma) \\ \vdots \\ \phi_c(\theta - (m-1)\gamma) \end{bmatrix}.$$

The dynamic equations of the electric motors can be obtained by using the following ‘‘Lagrangian’’ differential equation

$$\frac{d}{dt} \left(\frac{\partial K}{\partial \dot{\mathbf{q}}^T} \right) - \frac{\partial K}{\partial \mathbf{q}^T} = \mathbf{V}_e - \mathbf{R}_e \dot{\mathbf{q}} \quad (2)$$

where K is the Lagrangian function of the system, \mathbf{V}_e is the extended input vector and \mathbf{R}_e is the extended dissipating matrix. The power P_d dissipated in the system can be expressed as follows: $P_d = \dot{\mathbf{q}}^T \mathbf{R}_e \dot{\mathbf{q}}$. For electric motors, the Lagrangian K is function of the electric angle θ , but it is not a function of the electric charge \mathbf{Q} . For *multi-phase synchronous motors* the Lagrangian function K has the following structure:

$$K = \frac{1}{2} \dot{\mathbf{q}}^T \mathbf{L}_e \dot{\mathbf{q}} - \dot{\mathbf{q}}^T \Phi(\mathbf{q}) \quad (3)$$

where \mathbf{L}_e is the extended energy matrix of the system. In this case we have that:

$$\frac{d}{dt} \left(\frac{\partial K}{\partial \dot{\mathbf{q}}^T} \right) = \mathbf{L}_e \ddot{\mathbf{q}} - \frac{\partial \Phi}{\partial \mathbf{q}} \dot{\mathbf{q}}, \quad \frac{\partial K}{\partial \mathbf{q}^T} = -\frac{\partial \Phi^T}{\partial \mathbf{q}} \dot{\mathbf{q}}.$$

From (2) one obtains the dynamic equations of the system:

$$\mathbf{L}_e \ddot{\mathbf{q}} = \mathbf{V}_e - \mathbf{R}_e \dot{\mathbf{q}} - \left[\frac{\partial \Phi^T}{\partial \mathbf{q}^T} - \frac{\partial \Phi}{\partial \mathbf{q}} \right] \dot{\mathbf{q}}. \quad (4)$$

The term $\frac{\partial K}{\partial \dot{\mathbf{q}}^T}$ present in the left part of equation (2) represents the back electromotive voltage generated by the rotor movements. The last term of equation (4) is a skew-symmetric term which represents an internal energy redistribution. From (4) one directly obtains the differential equations of the motor:

$$\underbrace{\begin{bmatrix} \mathbf{L} & 0 \\ 0 & J_r \end{bmatrix}}_{\mathbf{L}_e} \underbrace{\begin{bmatrix} \dot{\mathbf{I}} \\ \dot{\omega}_r \end{bmatrix}}_{\dot{\mathbf{q}}} = - \underbrace{\begin{bmatrix} \mathbf{R} & \mathbf{K}_\tau(\theta) \\ -\mathbf{K}_\tau^T(\theta) & b_r \end{bmatrix}}_{\mathbf{R}_e + \mathbf{W}_e} \underbrace{\begin{bmatrix} \mathbf{I} \\ \omega_r \end{bmatrix}}_{\mathbf{q}} + \underbrace{\begin{bmatrix} \mathbf{V} \\ -\tau_e \end{bmatrix}}_{\mathbf{V}_e} \quad (5)$$

Matrices \mathbf{L}_e , \mathbf{R}_e and \mathbf{W}_e are defined as follows:

$$\mathbf{L}_e = \begin{bmatrix} \mathbf{L} & 0 \\ 0 & J_r \end{bmatrix}, \quad \mathbf{R}_e = \begin{bmatrix} \mathbf{R} & 0 \\ 0 & b_r \end{bmatrix}, \quad \mathbf{W}_e = \begin{bmatrix} 0 & \mathbf{K}_\tau(\theta) \\ -\mathbf{K}_\tau^T(\theta) & 0 \end{bmatrix}$$

where $\mathbf{K}_\tau(\theta)$ and \mathbf{R} are, respectively, the torque vector and the dissipating matrix of the motor:

$$\mathbf{K}_\tau(\theta) = \frac{\partial \Phi_c^T(\mathbf{q})}{\partial \theta}, \quad \mathbf{R} = p \begin{bmatrix} R_i \end{bmatrix}_{1:m} \quad (6)$$

and $\mathbf{L} > 0$ is the positive-definite inductance matrix:

$$\mathbf{L} = p \begin{bmatrix} L_1 & M_{12} & M_{13} & \cdots & M_{1m} \\ M_{12} & L_2 & M_{23} & \cdots & M_{2m} \\ M_{13} & M_{23} & L_3 & \cdots & M_{3m} \\ \vdots & \vdots & \vdots & \ddots & \vdots \\ M_{1m} & M_{2m} & M_{3m} & \cdots & L_m \end{bmatrix}. \quad (7)$$

Writing system (5) in a compact form one obtains:

$$\mathbf{L}_e \ddot{\mathbf{q}} = -\mathbf{R}_e \dot{\mathbf{q}} - \mathbf{W}_e \dot{\mathbf{q}} + \mathbf{V}_e.$$

System (5) can be graphically represented by the POG scheme shown in Fig. 4. The elaboration blocks present

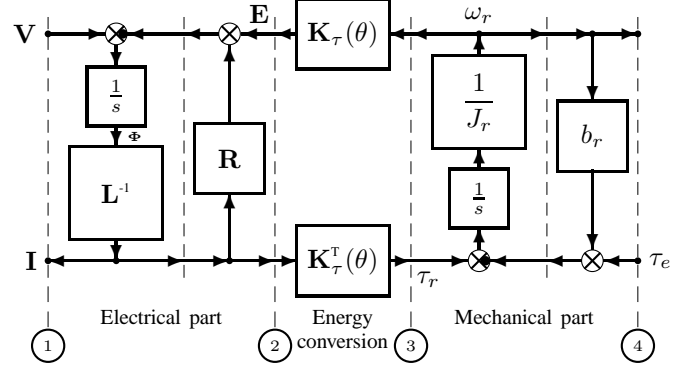


Fig. 4. POG scheme of the multi-phase electric motor.

between the power sections ① and ② represent the *Electrical part* of the system, while the blocks between sections ③ and ④ represent the *Mechanical part* of the system. The connection block between sections ② and ③ represents the conversion of energy and powers (without accumulation nor dissipation) between the electrical and mechanical domains. Function $\phi_c(\theta)$ is even and periodic of period 2π (see hypotheses H1 and H2) and therefore it can be developed in Fourier series of cosines with only odd harmonics:

$$\phi_c(\theta) = \varphi_c \bar{\phi}(\theta) = \varphi_c \sum_{n=1:2}^{\infty} a_n \cos(n\theta). \quad (8)$$

From (8) it follows that flux vector $\Phi_c(\theta)$ can be rewritten in a compact form as:

$$\Phi_c(\theta) = \varphi_c \left[\begin{array}{c} \sum_{n=1:2}^{\infty} a_n \cos[n(\theta - h\gamma)] \\ \vdots \\ \sum_{n=1:2}^{\infty} a_n \cos[n(\theta - h\gamma)] \end{array} \right]_{0:m-1}. \quad (9)$$

From (6), the torque vector $\mathbf{K}_\tau(\theta)$ can be expressed as follows:

$$\mathbf{K}_\tau(\theta) = p \varphi_c \left[\begin{array}{c} - \sum_{n=1:2}^{\infty} n a_n \sin[n(\theta - h\gamma)] \\ \vdots \\ - \sum_{n=1:2}^{\infty} n a_n \sin[n(\theta - h\gamma)] \end{array} \right]_{0:m-1}. \quad (10)$$

Let us now consider the following orthonormal transformation (see the generalized Concordia transformation in [4]):

$${}^t \mathbf{T}_\omega^T(\theta) = \omega \mathbf{T}_t(\theta) = \sqrt{\frac{2}{m}} \left[\begin{array}{c} \left[\begin{array}{c} \cos(k(\theta - h\gamma)) \\ \sin(k(\theta - h\gamma)) \end{array} \right]_{1:2:m-2}^h \\ \vdots \\ \left[\begin{array}{c} \frac{1}{\sqrt{2}} \end{array} \right]_{0:m-1}^h \end{array} \right].$$

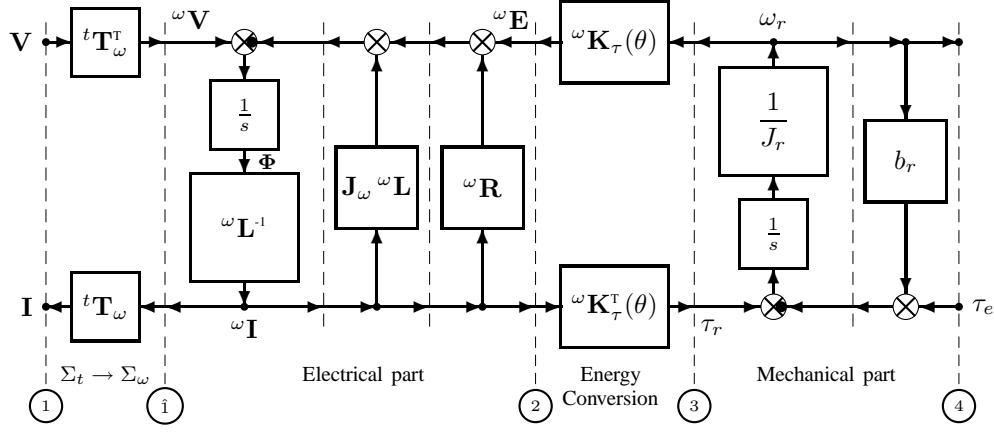


Fig. 5. POG scheme of a multi-phase electrical motor in the transformed space Σ_ω .

Matrix ${}^\omega\mathbf{T}_t(\theta)$ represents a multi-dimensional rotation in the state space, is a function of the electrical motor angle θ and transforms the electric variables \mathbf{V} and \mathbf{I} from the original reference frame Σ_t to a transformed rotating frame Σ_ω . Applying transformation ${}^\omega\mathbf{T}_t$ to matrices \mathbf{L} , \mathbf{R} and $\mathbf{K}_\tau(\theta)$, from (5) one obtains the transformed system:

$$\begin{bmatrix} {}^\omega\mathbf{L} & 0 \\ 0 & J_r \end{bmatrix} \begin{bmatrix} {}^\omega\dot{\mathbf{I}} \\ \dot{\omega}_r \end{bmatrix} = - \begin{bmatrix} {}^\omega\mathbf{R} + \mathbf{J}_\omega {}^\omega\mathbf{L} & {}^\omega\mathbf{K}_\tau \\ -{}^\omega\mathbf{K}_\tau^T & b_r \end{bmatrix} \begin{bmatrix} {}^\omega\mathbf{I} \\ \omega_r \end{bmatrix} + \begin{bmatrix} {}^\omega\mathbf{V} \\ -\tau_e \end{bmatrix} \quad (11)$$

where ${}^\omega\mathbf{I} = {}^\omega\mathbf{T}_t \mathbf{I}$, ${}^\omega\mathbf{V} = {}^\omega\mathbf{T}_t \mathbf{V}$, ${}^\omega\mathbf{R} = {}^\omega\mathbf{T}_t \mathbf{R} {}^t\mathbf{T}_\omega = \mathbf{R} = p R \mathbf{I}_m$ and ${}^\omega\mathbf{L} = {}^\omega\mathbf{T}_t \mathbf{L} {}^t\mathbf{T}_\omega$. Let the self and mutual induction coefficients of matrix \mathbf{L} be defined as $M_{ij} = M_0 \cos((i-j)\gamma)$, $L_i = \Delta_0 + M_0$ for $i, j \in \{1, 2, \dots, m\}$. The transformed matrix ${}^\omega\mathbf{L}$ has the following structure:

$${}^\omega\mathbf{L} = p \begin{bmatrix} \Delta_0 + \frac{mM_0}{2} & 0 & 0 & 0 & \dots & 0 \\ 0 & \Delta_0 + \frac{mM_0}{2} & 0 & 0 & \dots & 0 \\ 0 & 0 & \Delta_0 & 0 & \dots & 0 \\ 0 & 0 & 0 & \Delta_0 & \dots & 0 \\ \vdots & \vdots & \vdots & \vdots & \ddots & \vdots \\ 0 & 0 & 0 & 0 & \dots & \Delta_0 \end{bmatrix}$$

where Δ_0 and M_0 are proper positive parameters. The structure of transformed torque vector ${}^\omega\mathbf{K}_\tau(\theta)$ is the following:

$${}^\omega\mathbf{K}_\tau(\theta) = {}^\omega\mathbf{T}_t \mathbf{K}_\tau(\theta) = -p \varphi_c \sqrt{\frac{m}{2}} \cdot \begin{bmatrix} \sum_{n=0:2m}^k [(n+k) a_{n+k} + (n-k) a_{n-k}] \sin(n\theta) \\ \sum_{n=0:2m}^k [(n+k) a_{n+k} - (n-k) a_{n-k}] \cos(n\theta) \\ -\sqrt{2} \sum_{n=m:2m}^{\infty} n a_n \sin(n\theta) \end{bmatrix}. \quad (12)$$

Let $\omega = \dot{\theta} = p \theta_r$ denote the time-derivative of the electric

angle θ . The structure of matrix \mathbf{J}_ω in (11) is:

$$\mathbf{J}_\omega = \begin{bmatrix} \begin{bmatrix} 0 & -k\omega \\ k\omega & 0 \end{bmatrix} & 0 \\ 0 & 1:2:m-2 \\ 0 & 0 \end{bmatrix}.$$

The POG scheme describing the considered electrical motor in the transformed frame Σ_ω , see eq. (11), is shown in Fig. 5. If the m phases of the rotor are star-connected then the system reduces to order $m-1$. Note that vector ${}^\omega\mathbf{K}_\tau(\theta)$ is composed only by the harmonics $\sin(n\theta)$ and $\cos(n\theta)$ where n is an integer number multiple of $2m$. Vector ${}^\omega\mathbf{K}_\tau(\theta)$ can be easily computed knowing the coefficients a_n of the Fourier series of the rotor flux, see eq. (8). Let vector ${}^\omega\mathbf{K}_\tau(\theta)$ be rewritten in the following form:

$${}^\omega\mathbf{K}_\tau(\theta) = \begin{bmatrix} \begin{bmatrix} {}^\omega K_{kd}(\theta) \\ {}^\omega K_{kq}(\theta) \end{bmatrix} \\ 1:2:m-2 \\ {}^\omega K_m(\theta) \end{bmatrix}. \quad (13)$$

Remarks: 1) ${}^\omega K_{kd}(\theta)$ and ${}^\omega K_{kq}(\theta)$ are respectively ‘‘odd’’ and ‘‘even’’ periodic functions of frequency $\omega = 2m$; they are influenced by all the odd components a_i of the Fourier series of function $\bar{\phi}_c(\theta)$, except for $i \in \{m:2m:\infty\}$; 2) ${}^\omega K_{kq}(\theta)$ are the only components of vector ${}^\omega\mathbf{K}_\tau(\theta)$ whose mean value can be constant and different from zero; 3) the last component ${}^\omega K_m(\theta)$ is a periodic function of frequency $\omega = m$, ‘‘odd’’ with respect to θ , ‘‘even’’ with respect to $\theta + \frac{\pi}{2m}$ and influenced only by the components a_i , for $i \in \{m:2m:\infty\}$, of the Fourier series of the flux $\bar{\phi}_c(\theta)$. In Fig. 8 functions ${}^\omega \bar{K}_{kd}(\theta)$, ${}^\omega \bar{K}_{kq}(\theta)$ and ${}^\omega \bar{K}_m(\theta)$ are shown when the rotor flux $\bar{\phi}_c$ is odd-polynomial interpolated (see Fig. 6 where $\bar{\phi}_r(\alpha, \theta)$ is a polynomial of order r with only odd powers of θ) and sinusoidally interpolated (see Fig. 7). These are the functions given in (12) and (13), normalized with respect to the common coefficient $p\varphi_c \sqrt{\frac{m}{2}}$, referred to the case $m = 7$ and considering the Fourier series until harmonic $n = 1000$. Functions ${}^\omega \bar{K}_{kd}(\theta)$, for $k \in \{1:2:m-2\}$, are shown in the upper part of the two pictures of Fig. 8 (red for $k=1$, blue for $k=3$ and green for $k=5$). Function ${}^\omega \bar{K}_{1q}(\theta)$ has usually an amplitude greater

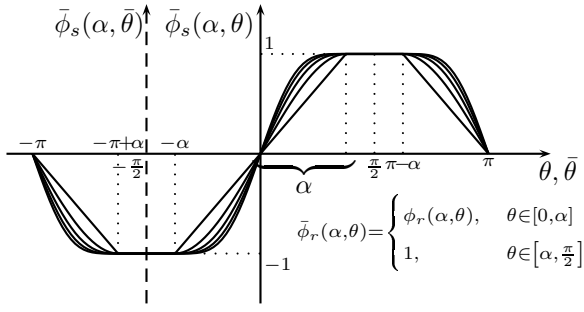


Fig. 6. Periodic signals $\bar{\phi}_r(\alpha, \theta)$ with odd-polynomial interpolation for $r \in \{1, 3, 5, 7, 9\}$.

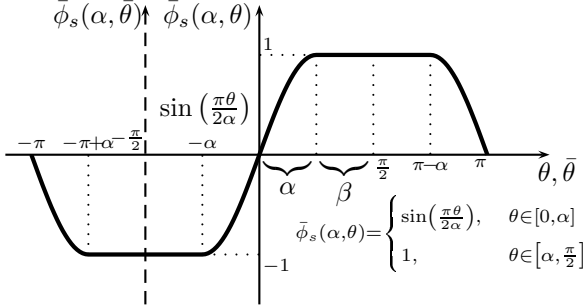


Fig. 7. Periodic signal $\bar{\phi}_s(\alpha, \theta)$ with sinusoidal interpolation.

than the other $\omega \bar{K}_{kq}(\theta)$. Function $\omega \bar{K}_m(\theta)$ is shown in the bottom part of the two pictures of Fig. 8. Note that, as stated in the *Remarks*, functions $\omega \bar{K}_{kd}(\theta)$ are *odd* and periodic with $\omega = 2m$, functions $\omega \bar{K}_{kq}(\theta)$ are *even* and periodic with $\omega = 2m$ and function $\omega \bar{K}_m(\theta)$ is *odd* with respect to θ , *even* with respect to $\theta + \frac{\pi}{2m}$ and with frequency $\omega = m$. The analysis of the components of torque vector $\omega \mathbf{K}_\tau$ is useful to calculate the optimal rotor flux that minimizes the currents needed to generate the desired torque, see [4] and [5].

Proposition: *the torque vector $\omega \mathbf{K}_\tau$ can be constant (not function of the electric angle θ) only for the flux functions $\bar{\phi}(\theta)$ which can be expressed in Fourier series as follows:*

$$\bar{\phi}(\theta) = \sum_{i=1:2}^{m-2} a_i \cos(i\theta). \quad (14)$$

All the constant components of the torque vector $\omega \mathbf{K}_\tau(\theta)$ can be obtained for $n = 0$:

$$\omega \mathbf{K}_\tau^T(\theta)|_{n=0} = -\varphi_c p \sqrt{\frac{m}{2}} \begin{bmatrix} \left[\begin{array}{cc} 0 & k a_k \end{array} \right]_k \\ \left[\begin{array}{cc} 0 & k a_k \end{array} \right]_{1:2:m-2} \end{bmatrix}. \quad (15)$$

Main Result: *among all the fluxes providing a constant vector $\omega \mathbf{K}_\tau$, the one that minimizes the module of the current vector \mathbf{I} (and therefore the dissipated power) is given by:*

$$\bar{\phi}(\theta) = \cos((m-2)\theta). \quad (16)$$

In Fig. 9 a schematic representation of the optimal flux is given in the case of seven-phase motor with single polar expansion. In this case the optimal shape of flux $\bar{\phi}(\theta)$ is a cosine function of frequency $\omega = m-2 = 5$.

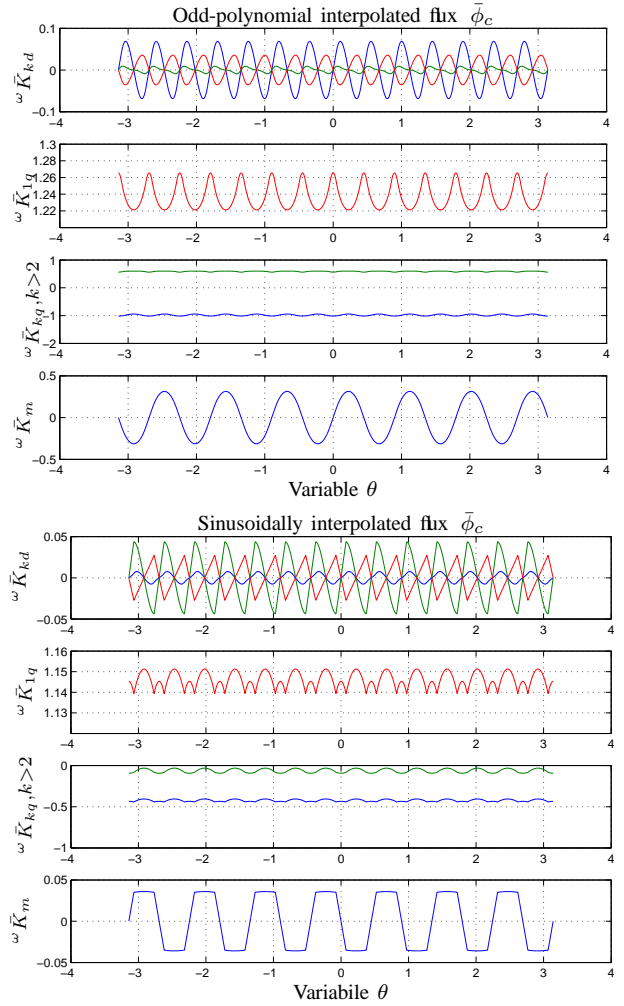


Fig. 8. Functions $\omega \bar{K}_{kd}(\theta)$, $\omega \bar{K}_{kq}(\theta)$ and $\omega \bar{K}_m(\theta)$, for $m = 7$ (red for $k = 1$, blue for $k = 3$, green for $k = 5$), when the rotor flux $\bar{\phi}_c$ is odd-polynomial interpolated ($r = 5$, $\alpha = \frac{\pi}{5}$) and sinusoidally interpolated ($\alpha = \frac{\pi}{3}$).

IV. SIMULATIONS

The model of the motor in the case of seven-phase star-connected motor has been implemented in Matlab/Simulink. The Simulink scheme clearly reflects the POG structure (see Fig. 5) and it needs only standard blocks as integrator, gain, adder. The simulation results presented in this Section have been obtained with the following electrical and mechanical parameters: $m = 7$, $p = 1$, $R = 3\Omega$, $L_0 = 0.1$ H, $M_0 = 0.08$ H, $N_c = 100$, $N_a = 200$ (number of considered harmonics in the Fourier series), $\varphi_r = 0.02$ W, $J_r = 1.6$ kg m², $b_r = 0.8$ Nm s/rad, $\tau_e = 0$. The torque τ_r generated by current vector $\omega \mathbf{I}$ is given by $\tau_r = \omega \mathbf{K}_\tau \omega \mathbf{I}$, see Fig. 5. A constant torque τ_r is obtained for all current vectors $\omega \mathbf{I}$ satisfying relation $\omega \mathbf{I} = \omega \mathbf{I}_0 + \text{Ker}[\omega \mathbf{K}_\tau]$ where $\omega \mathbf{I}_0$ is a particular solution of the considered relation $\tau_r = \omega \mathbf{K}_\tau \omega \mathbf{I}$. Among all these vectors $\omega \mathbf{I}$ the one with the minimum modulus is $\omega \mathbf{I}_{des} = \frac{\tau_d}{|\omega \mathbf{K}_\tau|} \omega \hat{\mathbf{K}}_\tau$ parallel to $\omega \mathbf{K}_\tau$ ($\omega \hat{\mathbf{K}}_\tau$ is the versor and τ_d is the desired torque). Among all the fluxes given by (14), the one that minimizes the modulus of the minimum current $\omega \mathbf{I}_{des}$ is the one which

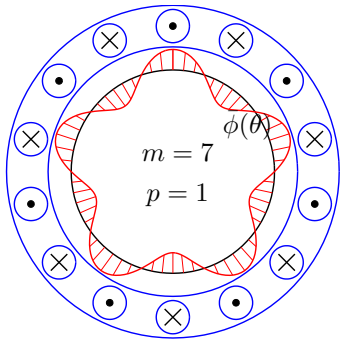


Fig. 9. Shape of the rotor flux $\bar{\phi}(\theta)$ when $m = 7$ and $p = 1$.

maximizes the modulus of vector ${}^\omega \mathbf{K}_\tau$ under the constraint of unitary maximum amplitude of the flux function $\bar{\phi}(\theta)$. The considered input voltage in the transformed reference frame is: ${}^\omega \mathbf{V}_0 = ({}^\omega \mathbf{R} + \mathbf{J}_\omega {}^\omega \mathbf{L}) {}^\omega \mathbf{I}_{des} + {}^\omega \mathbf{K}_\tau \omega_r$. Fig. 10 shows the phase currents in the transformed reference frame for different shapes of rotor flux: sinusoidal (black dotted line), 3-rd harmonic (blue dashed line), 5-th harmonic (red solid line), sinusoidal interpolation (green solid line), odd-polynomial interpolation (magenta dash-dotted line), when the desired current ${}^\omega \mathbf{I}_{des}$ is calculated from the desired torque $\tau_d = 10$ Nm. The minimum current (the red solid line in Fig. 10) is achieved using the optimal flux given by the above relation (in this case it is the fifth harmonic). Motor velocity ω_m and generated torque τ_m for different types of rotor flux are shown in Fig. 11. The 1-st, 3-rd and 5-th harmonics of direct and quadrature currents ${}^\omega \mathbf{I}_d$ and ${}^\omega \mathbf{I}_q$ in Σ_ω reference frame are shown in Fig. 12 and Fig. 13.

V. CONCLUSIONS

In this paper a m -phase permanent magnet synchronous motor has been modelled using the Power-Oriented Graphs (POG) technique. This approach exhibits some advantages in comparison with other graphical techniques and allows to realize very compact schemes which can be easily translated into Simulink models. The optimal shape of the rotor flux which minimizes the module of the current vector has been provided thanks to a deep analysis of the torque vector. Simulations show the effectiveness of the realized model in the case of a seven-phase star-connected motor.

REFERENCES

- [1] R. Zanasi, "Power Oriented Modelling of Dynamical System for Simulation", IMACS Symp. on Modelling and Control of Technological System, Lille, France, May 1991.
- [2] Zanasi R., "Dynamics of a n -links Manipulator by Using Power-Oriented Graph", SYROCO '94, Capri, Italy, 1994.
- [3] E. Semail, X. Kestelyn, A. Bouscayrol, "Right Harmonic Spectrum for the Back-EMF Force of a n -phase Synchronous Motor", Industry Applications Conference, 2004, 39th IAS Annual Meeting
- [4] R. Zanasi, F. Grossi "The POG technique for modelling multi-phase permanent magnet synchronous motors", 6th EUROSIM Congress on Modelling and Simulation, Ljubljana, 9-13 September 2007.
- [5] R. Zanasi, F. Grossi "Optimal Rotor Flux Shape for Multi-phase Permanent Magnet Synchronous Motors", accepted by 13th International Power Electronics and Motion Control Conference, September 1-3 2008, Poznan, Poland.

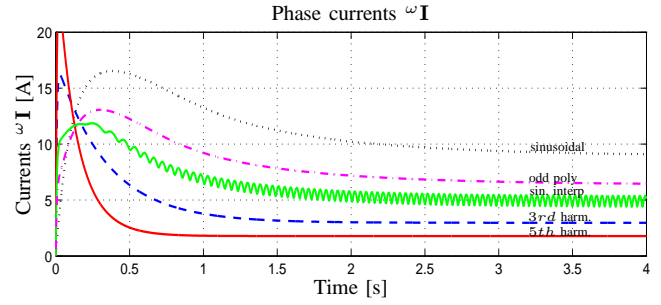


Fig. 10. Phase currents ${}^\omega \mathbf{I}$ in the transformed reference frame for different shapes of rotor flux.

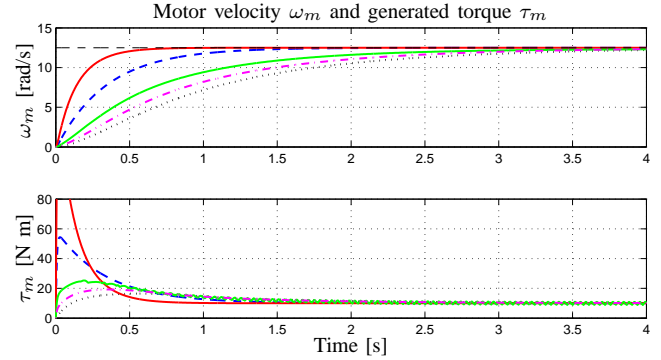


Fig. 11. Motor velocity ω_m and generated torque τ_m for different types of rotor flux.

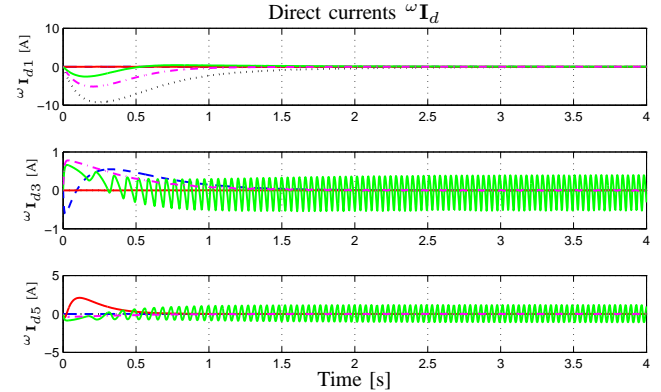


Fig. 12. First, third and fifth harmonics of direct currents ${}^\omega \mathbf{I}$ in the transformed Σ_ω reference frame.

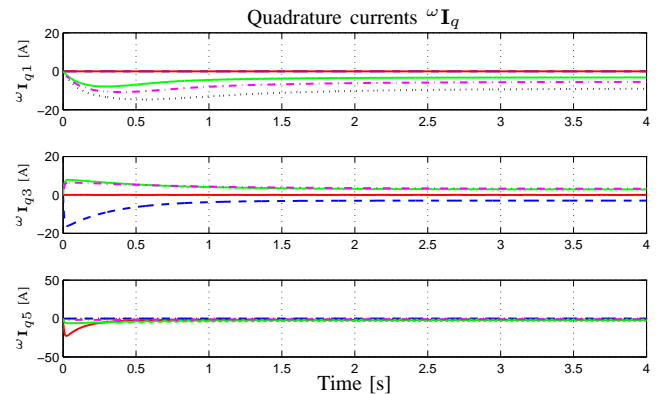


Fig. 13. 1st, 3rd and 5th harmonics of quadrature currents ${}^\omega \mathbf{I}$ in the transformed Σ_ω reference frame.